INFLUENCE OF SUBSTRATE SURFACE ROUGHNESS ON THE THERMAL EMISSIVITY OF TITANIUM CARBIDE COATINGS ON GRAPHITE

Kalapala Prasad[1], Thengiri Maharaja Pillai Subbulakshmi[2], Paramasivam Premkumar[3], S. Ravishankar[4], Ismail Hossain[5], Sami Al Obaid[6], Md. Abul Kalam[7], Thangarajan Sivasankaran Senthilkumar[8] and Chathapuram Balasubramanian Priya[9]

[1] Department of Mechanical Engineering, Jawaharlal Nehru Technological University College of Engineering Kakinada (Univercity College of Engineering in JNTU Kakinada), Andhra Pradesh 533003, India. Prasadkalapala567@gmail.com

[2] Department of Marine Engineering, Noorul Islam Centre For Higher Education, Kumaracoil, Tamil Nadu 629180, India. reachtss@gmail.com

[3] Department of Mechanical Engineering, St.Joseph's College of Engineering, OMR, Chennai, Tamil Nadu 600119, India. prem1125@gmail.com

[4] Department of Mechanical Engineering, KPR Institute of Engineering and Technology, Coimbatore, Tamil Nadu 641407 India. phanendra51@gmail.com

[5] School of Natural Sciences and Mathematics, Ural Federal University, Yekaterinburg, 620000, Russia. hossain.ismail44@yahoo.com

[6] Department of Botany and Microbiology, College of Science, King Saud University, PO Box -2455, Riyadh -11451, Saudi Arabia. sami907@gmail.com

[7] School of Civil and Environmental Engineering, FEIT, University of Technology Sydney, NSW 2007, Australia. makalam.phd@outlook.com

[8] Department of Mechanical Engineering, K. Ramakrishnan College of Technology, Tiruchirappalli – 621 112, India.

[9] Department of Mechanical Engineering, OASYS Institute of Technology, Tiruchirappalli, Tamil Nadu, 621006, India

Abstract

This study focused on the impact of substrates shape on the heat radiationcharacteristics of a coating made of titanium carbide (TiC) deposited over a graphite basis. TiC coating emissivity increase by 29.65% at 1050°C and by 37.45% at 1650 °C when graphite (Gr) substrate surface roughness (Ra) was decreased from 3.01 µm to 0.73 µm. Simultaneously, the TiC coating's spectrum emissivity on the graphite substrate indicated the material's clear characteristic

heat radiation. These findings demonstrated that the coating and substrate interacted to determine the coating's heat radiation properties. A simplified coating model created to consider how the shape of the substrate affects the coating's ability to conduct heat. Ultimately, the rough form of the substrate led to a decrease in the coating's heat radiation characteristics and an enhancement in energy loss at the interface.

Keywords: Heat radiation, Emmissivity, graphite, substrate, Temperature, TiC.

1 Introduction

Titanium Carbide, or TiC, is a vital ceramic substance used in many different military and civilian applications[1]. It is a highly desirable material due to its high specific strength and modulus as well as its low thermal expansion and strong thermal conductivity. In applications like solar cell film, wear-resistant coating, anti-oxidation coating for preservatives, and so forth, coatings or films are crucial forms of titanium carbide[2]. TiC coatings are frequently used in high-temperature environments when in use, for as in industrial heat exchangers or thermal protection systems used in aircraft and spacecraft [3]. To prevent oxide etch in passive heating systems like thermal protection systems, TiC coating is frequently used as the layer of barrier. In this situation, heat is transferred through the coating to the underlying material[4].

Heat is transferred from the graphite components to the TiC coating, with the flow direction being from the substrate to the coating. The heat transmission properties of a coating are influenced by a number of factors, including the coating itself, the substrate, the interface's thermal resistance, and the coating's proximity to other heat sources[5]. Notably, at elevated temperatures, heat radiation becomes the main mechanism governing the exchange of heat between materials and their environment.

TiC emits an electromagnetic field due to the random thermal mobility of its electrons, which is known as heat radiation. A material's infrared emissivity is a key property for defining its heat radiation properties[6]. A substance's emissivity could be calculated by contrasting its own emission intensity with that of a black body. The Stefan-Boltzmann equation states that heat radiation rises rapidly with temperature, particularly at maximum temperatures[4], [7].

So, the heat radiation attributes of a TiC coating substantially affect heat transfer and the temperature distribution across components. When the substrate and coating share identical chemical compositions and thicknesses, it is their respective morphologies that most significantly influence the coating's heat radiation efficiency[8]. Heat radiation correlations with coating surface features such roughness, existence of an oxide layer, and contaminants have been the subject of a large body of theoretical and empirical research. The influence of surface shape on emissivity has been demonstrated using a number of models. To illustrate the connection between surface roughness and emissivity, for instance, the researchers presented an equation and a model for approximation[9], [10].

The analysis of absorptivity and emissivity in the context of surface roughness, with feature sizes comparable to the wavelength of interest, has been categorized into three distinct regimes. For ceramics composed of ZrB_2 with 15% TiC, the machined surface pattern has been shown to considerably influence heat radiation at temperatures below 1550K. A number of mathematical models have also been developed to articulate the correlation between the surface morphology and its heat radiation properties[11]. Nonetheless, a dearth of research has examined how the substrate affects emissivity when examining the coating's heat radiation characteristics. There was a significant degree of interference at the substrate-coating interface when heat flowed from the substrate to the coating. Related studies have demonstrated that substrate morphologies and composition significantly influence the coating's heat radiation when coating thicknesses range from a few microns to tens of microns [12].

Using a Ni alloy substrate, researchers [13] studied how changing the substrate shape affected the heat radiation parameters of an Au film. The findings demonstrated that raising the substrate roughness led to the destruction of Au film integrity in addition to an increase in effective surface emitting area [14]. The majority of studies disregarded the substrate's impact on the coating's characteristics related to heat radiation. In the current work, chemical vapour deposition was used to create a TiC coating on three distinct morphologies of graphite substrates. Researchers looked into how substrate morphology affected heat radiation characteristics measured from the TiC coating. There was also discussion of the substrate-coating heat transmission methods. To attempt a detailed analysis of the physical phenomena involved, a basic model had been developed.

2 Materials and methods

2.1 Preparation of material

The high purity graphite was sliced onto a substrate measuring 10 mm x 10 mm x 2 mm for a TiC deposit. To get the graphite substrates ready for the TiC coating, they were polished using progressively finer grit abrasive papers. Sample X was a graphite substrate polished with 400 grit TiC, Sample Y was polished with 1550 grit TiC, and Sample Z was polished with W0.5 emery grinding grease. Following polishing, acetone and methanol were used in an ultrasonic cleaner to clean the graphite substrates. Following the drying of the graphite substrates, chemical vapour deposition (CVD) was used to provide a TiC coating on the substrate surface. During the deposition process for TiC coating, hydrogen served as the carrier gas to introduce methyltrichlorosilane (MTS, CH_3SiCl_3) into the furnace. The deposition rate of the TiC coating was also controlled by using argon as a diluent gas. The deposition furnace's temperature was regulated between 950 and 1050°C during the deposition process. To achieve the intended coating thickness in this study, the deposition duration was regulated to 240 hours.

2.2 Properties and its extents

In this research, the heat radiation of samples was measured in a direct fashion. As can be seen in Fig. 1, an apparatus for measuring emissivity at high temperatures was employed. The main vacuum element of the system consisted of a turbomolecular pump connected in series with a mechanical pump. This setup was established to achieve an extremely low air pressure (around

10−410−4 mbar), with the aim of preventing any atmospheric turbulence. When samples were placed inside the inductance coil, they were heated by the induction furnace.

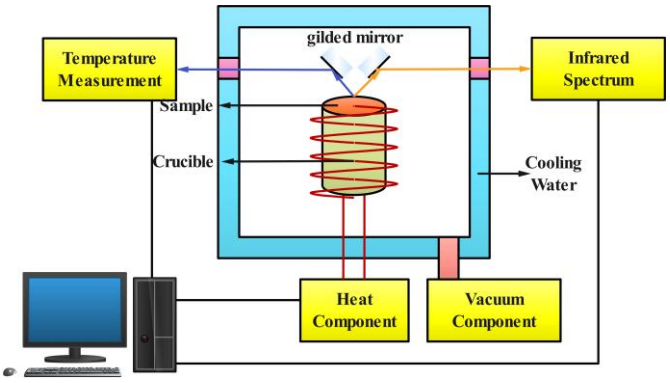

Figure. 1 Diagrammatic representation of the heat radiation detection system

The mechanism for temperature monitoring was responsible for tracking the temperature levels of the sample. The infrared radiation signals emitted by the heated sample were detected using a Fourier transform infrared spectrometer (FTIR) equipped with a mercury cadmium telluride (MCT) detector. The samples' spectral emissivity was determined by comparing their heat radiation spectra to that of a blackbody standard[15], [16].

$$\varepsilon(\lambda,T) = \frac{L_s(\lambda,T)}{L_b(\lambda,T)} \qquad (1)$$

where Ls(λ,T) and Lb(λ,T) stood for the sample's and the blackbody's respective heat radiation intensities at a given wavelength (λ) and temperature (T). A straightforward computation of heat radiation spectrograms could yield Ls(λ,T). Plank's Law provided the Lb(λ,T) calculation formula, which is displayed below[17]:

$$L_b(\lambda,T) = \frac{C_1}{\lambda^5\left[\exp\left(\frac{C_2}{\lambda T}\right)-1\right]} \qquad (2)$$

where the first radiation constant, C1 = 3.742 × 10–16 W·m^2, and the second, C2 = 1.439 × 10^{-2} W·K, were measured.

2.3 Evaluation of total emissivity

The ability to radiate heat over the studied wavelength range was characterised by the total emissivity, which was determined by integrating the emissivity across the spectrum. As per [18], the total emissivity was obtained by integrating the spectral emissivity ελ from λ1 to λ2.

$$\varepsilon_T = \frac{\int_{\lambda_1}^{\lambda_2} \varepsilon_\lambda E_{b\lambda} d\lambda}{\int_{\lambda_1}^{\lambda_2} E_{b\lambda} d\lambda} = \frac{\sum_{\lambda_1}^{\lambda_2} \varepsilon_\lambda E_{b\lambda} \Delta\lambda}{\sum_{\lambda_1}^{\lambda_2} E_{b\lambda} \Delta\lambda} \qquad (3)$$

where

λ wavelength

T temperature.

Ebλ blackbody's heat radiation intensity

Coating was identified using X-ray diffraction (XRD) analysis using Cu Kα radiation. The information was recorded digitally from 20° to 80°of angle (2θ).

3 Results and discussions

The laser scanning confocal microscope measurements of the graphite substrate's surface roughness are shown in Table 1. The surface roughness decreased from 3.01μm to 0.73μm between substrates X and Z. The cross-sectional shape of a TiC coating on a graphite substrate. The coating is compact and has a thickness of approximately 20 μm. As a result, the coating qualifies as the perfect homogenous coating.

Table. 1 Roughness of the surface of Gr substrates

Substrate	Surface Roughness (μm)	Polishing grit
X	2.96 ± 0.13	400#
Y	1.28 ± 0.11	1550#
Z	0.69 ± 0.08	W0.5#

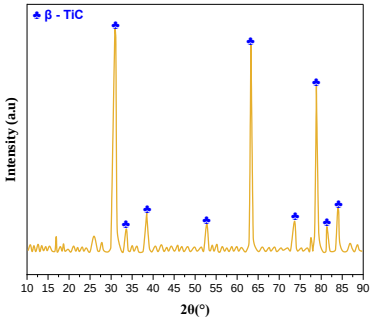

Figure. 2 The Coating's XRD Pattern

Simultaneously, the XRD data reveal that the coating's primary component is β-TiC. (Fig. 2). Sample Z has an interface that is quite smooth and free of defects. As thus, the substrate morphology dominated both the interface morphology and the interface bonding station. Ultimately, the heat transfer between the substrate and coating will be directly impacted by changes in the interface combination state.

Samples X, Y, and Z's spectral emissivity at 1050 and 1350˚C are displayed in Figure 3. The 10–14 μm spectrum emissivity curvatures of all three specimen follow the classic "V-pattern" mode, with a dip in intensity followed by a rise. The spectral emissivity has a minimum value of 12.5 μm and a maximum value of around 10 μm. The spectral emissivities of samples X and Y differed significantly in this wavelength range, although Sample Y and Z's discrepancies were less pronounced. In accordance with the single Lorentz oscillator model, TiC's infrared

emissivity exhibited unique variations in the 10–14 μm wavelength range. The Reststrahlen Zone of TiC is the name given to this unique region of spectral emissivity. The three samples' spectral emissivity displayed the TiC Reststrahlen Zone, indicating that the coating's heat radiation was mostly influenced by its material composition. Therefore, it could be concluded that the substrate was mostly responsible for the variations in spectral emissivity seen in the samples. At the same wavelength, SamplesX and Z's spectral emissivity increased as their substrate surface roughness decreased. Additionally, the samples' spectral emissivity varied with wavelength, with values ranging from 8-12 μm to 16-18 μm.

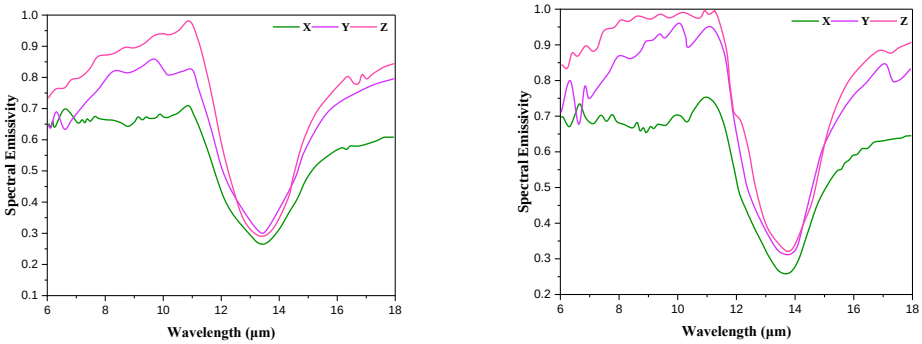

Figure. 3 Three samples with distinct substrate morphologies were analysed for their spectral emissivity: (a) 1050°C; (b) 1350°C

Sample X's spectral emissivity varied very little with wavelength. Both Sample Y and Z showed an increase in spectral emissivity with increasing wavelength in the aforementioned two wavebands, however Sample Z grew at a faster pace. As the temperature was increased from 1050 to 1350 °C, the spectral emissivity at the test wavelength increased in all samples. As temperature was raised, the gap between X and Y samples expanded in terms of their spectrum emissivity. Three samples were prepared for TiC coating in this work using the same depositional conditions. As a result, it is possible to regard the coating's chemical composition, thickness, and surface shape as being identical across samples. The morphology of the substrate was the sole variable. Consequently, it is possible to draw the conclusion that the substrate shape significantly influenced the TiC coating's spectral emissivity. The spectral emissivity differential grew as the temperature rise, amplifying these effects.

Figure 4 displays the variation of total emissivity as a function of temperature, ranging from 1050 to 1650 °C, for the three materials under study. The diagram indicates that the average emissivity of the three samples rises at lower temperatures and subsequently declines at higher temperatures. The heat radiation characteristics, as described by infrared radiation theory, are primarily governed by factors such as carrier density, carrier mobility, and the frequency of carrier collisions [19]. As the measurement temperatures increased, the activity of carriers enhanced the electromagnetic energy that the materials were emitting. Materials with higher energy emissions have better heat radiation capabilities. The failure to account for the substrate's effect on the heat radiation property is largely to responsible for this discrepancy. But in this investigation, the substrate was treated like any other part of the heat conduction system.

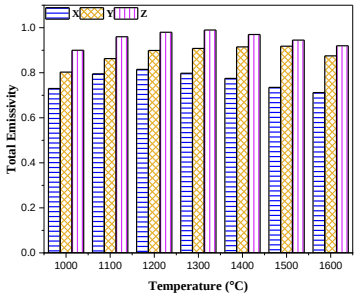

Figure. 4 Variation in temperature-dependent total emissivity of three samples

The structural configuration was envisioned with the substrate and the coating acting as layers in a composite structure. Given that the TiC coating and the graphite substrate expanded and contracted at dissimilar rates, stress occurred at their boundary. At the elevated temperatures in question, interfacial tension was considered minimal, allowing for efficient heat transfer from the substrate to the coating. Consequently, as the coating's temperature rise, its heat radiation initially increased. However, as temperature climbed during measurements, the escalating interfacial stress caused the interface to separate. Due to defects at the interface, heat was reflected more and transferred less efficiently from the substrate to the coating, reducing the coating's radiative capacity. Ultimately, this reduction manifested as a lower overall emissivity of the sample at high temperatures.

Moving from Sample X to Sample Z, there was a reduction in substrate roughness, which correspondingly led to a decrease in the interfacial resistance to heat flow. This change facilitated a rise in the overall emissivity and resulted in Sample Y and Sample Z exhibiting similar patterns of variation in emissivity at the transition temperature. In line with the overall trend observed in the spectral emissivity, the total emissivity augmented from Sample X to Sample Z with the diminishing roughness of the substrate. When contrasted with Sample X, the emissivity growth rates for Samples Y and Z were notably higher, registering increases of 11.67% at 1050 °C for Sample Y and 29.65% for Sample Z, respectively. Increasing test temperatures were associated with a faster increase in total emissivity, indicating that substrate shape was more important than temperature in determining the heat radiation characteristics of TiC.

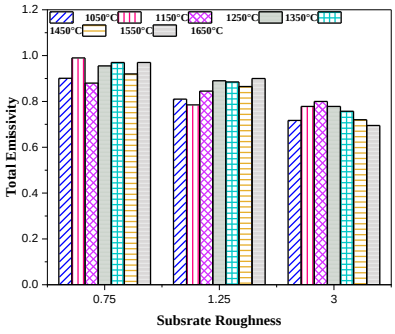

Figure.5 Samples' overall emissivity in relation to substrate roughness

Figure 5 illustrates the relationship between emissivity at various temperatures and substrate roughness for the three different samples. The graph shows that the total emissivity of the samples decreases in an almost linear fashion with the increase in substrate roughness, regardless of the temperature. A model is presented to encapsulate this nearly linear relationship between the total emissivity and the substrate roughness[20]:

$$E = a * x + b \qquad (4)$$

In the given relationship, E represents the total emissivity, while a and b are constants that characterize the influence of surface roughness on emissivity, with x being the variable representing surface roughness. Here, a surface roughness (x) of 0 corresponds to the emissivity of the coating on an ideally smooth graphite substrate, as suggested by the intercept b. The constant a quantifies the effect that the substrate's roughness has on the coating's ability to emit heat radiation.

The constants a and b at various temperatures are determined using the relationship between surface roughness and total emissivity as outlined in formula (4), with the findings. If the absolute value of a goes up, it means that the substrate roughness is having an increasingly detrimental effect on the heat radiation emitted by the TiC layer.

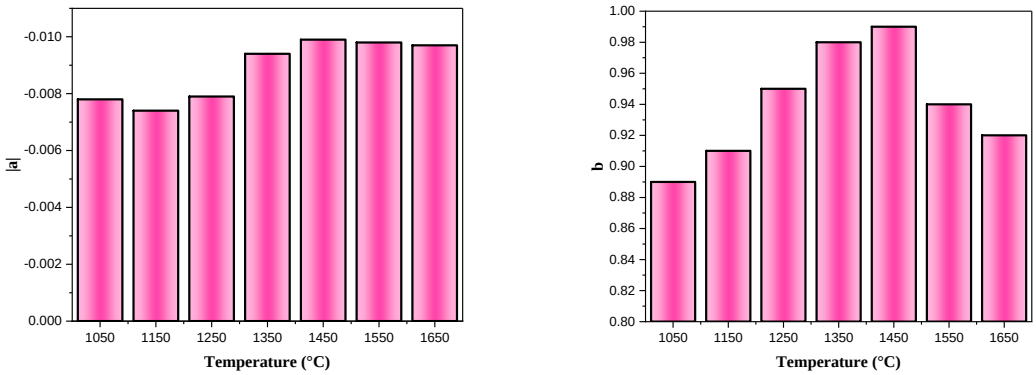

Figure . 6 The (a) results of a in absolute terms, (b) the variation of b with respect to temperature

Figure 6 shows the a and b absolute values at the measured temperatures. The rising tendency continues until a temperature of roughly 1450 °C is achieved, after which the absolute values start to fall. As shown by the variation of, the shape of the substrate has a large impact on the TiC coating's heat radiation below 1450 °C but a less impact above this temperature. Similar to the parameter |a|, the value of b increased and decreased as temperature did. As previously indicated, b had to do with the coating's heat radiation on the perfect smooth surface of the graphite substrate. The variations of a and b with temperature showed that there was a strong temperature dependence for the substrate's influence on the coating.

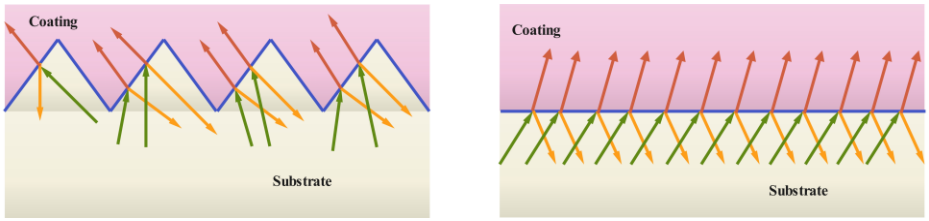

Figure .7 The heat transfer schematic among the substrate and coating (a) the smooth surface; (b) the rough surface

The heat radiation characteristic of a given coating is influenced by the properties of both the substrate it's applied to and the coating material itself. Figure 7 illustrates the coating diagram for two substrates that have either smooth or rough surface textures. For determining the apparent emissivity of a uniform coating within a layered structure, the researchers have deduced the following computational formula:

$$\varepsilon(\lambda) = (1-\rho) - \frac{\chi(1-\rho)^2}{e^{2\alpha d} - \rho\chi} \qquad (5)$$

where

d coating thickness

μ wavelength

ρ coating reflectivity

χ substrate reflectivity

a Lambert-Law Beer's absorption coefficient.

This formula showed a strong correlation between the coating's thickness, interface reflectivity, and coating reflectivity and its heat radiation property. The heat radiation from the substrate might pass through the coating if it was within a specific range. Thus, it was not possible to ignore the substrate's impact on the coating's heat radiation in this investigation .

The electromagnetic wave responsible for heat radiation experienced reflection, scattering, and refraction at the interface during transmission, as per the geometric optics principle. The heat radiation was dissipated as electromagnetic waves travelled from the substrate to the coating and interacted at the interface. In terms of power transfer, the contact area between the two materials can be compared to their thermal resistance. If the coating had been applied to a smooth surface, the potential for heat absorption by the coating could have been higher. A rougher interface between the substrate and the coating alters the heat transfer characteristics by increasing the surface area at the interface and the loss of energy in the heat flow. It implied that the coating's ability to radiate energy diminished as it reached thermal equilibrium, thereby lessening the coating's capacity to radiate heat. As a result, as substrate roughness increased, TiC coating's heat radiation property dropped.

4 Conclusions

TiC coatings were placed on graphite substrates of varying morphologies for this study in order to determine how the substrate's form affects the coatings' heat radiation qualities. It was observed that both the spectral and overall emissivity of the TiC coatings were inversely related to the roughness of the substrate. Furthermore, the effect of the substrate morphologies on the coating's ability to radiate heat was more pronounced at temperatures below 1450 °C and diminished at temperatures above this threshold. Further investigation showed that the TiC coating's heat radiation qualities had degraded because of the rough interface. This roughness led to increased energy dissipation and more complex interactions with electromagnetic waves.

Acknowledgments:

This project was supported by Researchers Supporting Project number (RSP2023R315) King Saud University, Riyadh, Saudi Arabia.The research funding from the Ministry of Science and Higher Education of the Russian Federation (Ural Federal University Program of Development within the Priority-2030 Program) is gratefully acknowledged.

References

[1] G. Sathiaraj, R. Mani, M. Muthuraj, and S. Mayakannan, “The mechanical behavior of Nano sized Al2O3 -reinforced Al-Si7-Mg alloy fabricated by powder metallurgy and forging,” *ARPN Journal of Engineering and Applied Sciences*, 11, 9, pp. 6056–6061, 2016.

[2] A. K. Singh, I. R. Khan, S. Khan, K. Pant, S. Debnath, and S. Miah, “Multichannel CNN model for biomedical entity reorganization,” *Biomed Res Int*, 2022.

[3] A. U. Haq *et al.*, “IIMFCBM: Intelligent integrated model for feature extraction and classification of brain tumors using MRI clinical imaging data in IoT-healthcare,” *IEEE J Biomed Health Inform*, 26, 10, pp. 5004–5012, 2022.

[4] R. Girimurugan, M. A. Logesh Kumar, B. Manikandan, C. Shilaja, and S. Mayakannan, “Static and Total Pressure Analysis of Three Way Catalytic Convertor using CFD,” 2022, pp. 7381–7387.

[5] N. S. Akbar, Z. Iqbal, B. Ahmad, and E. N. Maraj, “Mechanistic investigation for shape factor analysis of SiO2/MoS2-ethylene glycol inside a vertical channel influenced by oscillatory temperature gradient,” *Can J Phys*, 97, 9, pp. 950–958, 2019.

[6] S. Khan, “Business Intelligence Aspect for Emotions and Sentiments Analysis,” *First International Conference on Electrical, Electronics, Information and Communication Technologies (ICEEICT)*, IEEE, 2022, pp. 1–5, 2022.

[7] R. Girimurugan *et al.*, “Application of Deep Learning to the Prediction of Solar Irradiance through Missing Data,” *International Journal of Photoenergy*, 2023.

[8] F. S. Bayones, W. Jamshed, S. H. Elhag, and M. Rabea Eid, “Computational Galerkin Finite Element Method for Thermal Hydrogen Energy Utilization of First Grade Viscoelastic Hybrid Nanofluid Flowing Inside PTSC in Solar Powered Ship Applications,” *Energy and Environment*, 34, 4, pp. 1031–1059, 2023.

[9] S. Khan *et al.*, “BiCHAT: BiLSTM with deep CNN and hierarchical attention for hate speech detection,” *Journal of King Saud University-Computer and Information Sciences*, 34, 7, pp. 4335–4344, 2022.

[10] R. Almakki, L. AlSuwaidan, S. Khan, A. R. Baig, S. Baseer, and M. Singh, “Fault Tolerance Byzantine Algorithm for Lower Overhead Blockchain,” *Security and Communication Networks*, 2022.

[11] B. Ramesh, S. Sathish Kumar, A. H. Elsheikh, S. Mayakannan, K. Sivakumar, and S. Duraithilagar, “Optimization and experimental analysis of drilling process parameters in radial drilling machine for glass fiber/nano granite particle reinforced epoxy composites,” *Mater Today Proc*, 62, pp. 835–840, 2022

[12] D. Dinesh Kumar *et al.*, “Study of Microstructure and Wear Resistance of AA5052/B4C Nanocomposites as a Function of Volume Fraction Reinforcement to Particle Size Ratio by ANN,” *J Chem*, 2023.

[13] M. Tayyab, A. Hussain, M. A. Alshara, S. Khan, R. M. Alotaibi, and A. R. Baig, “Recognition of Visual Arabic Scripting News Ticker From Broadcast Stream,” *IEEE Access*, 10, pp. 59189–59204, 2022.

[14] S. Ahmad *et al.*, “Deep Learning Enabled Disease Diagnosis for Secure Internet of Medical Things,” *Computers, Materials & Continua*, 73, 01, pp. 965–979, 2022.

[15] Y. Guo, W. Xia, Z. Hu, and M. Wang, “High-temperature sensor instrumentation with a thin-film-based sapphire fiber,” *Appl Opt*, 56, 8, pp. 2068–2073, 2017.

[16] K.-K. Choi, P. Oduor, and A. Dutta, “Wavelength-selective thermal meta-emitters for thermophotovoltaic power generation,” in *Proceedings of SPIE - The International Society for Optical Engineering*, 2023

[17] A. Chirumamilla *et al.*, “Spectrally selective emitters based on 3D Mo nanopillars for thermophotovoltaic energy harvesting,” *Materials Today Physics*, 21, 2021.

[18] E. Brodu and M. Balat-Pichelin, “Emissivity of boron nitride and metals for the solar probe plus mission,” *J Spacecr Rockets*, 53, 6, pp. 1119–1127, 2016.8683fd76bd40f3d5b29c2e08ac9c0

[19] M. Yaseen, S. K. Rawat, and M. Kumar, “Analysis of MoS2-SiO2/water hybrid nanofluid flow with linear and quadratic thermal radiation induced by a stretching/shrinking surface

in a darcy–forchheimer porous medium," *Special Topics and Reviews in Porous Media*, 13, 5, pp. 31–48, 2022.

[20] J. Zhang, Y. Shang, X. Li, Y. Dong, and Y. Pei, "A novel technique for full-field deformation and temperature measurement by ultraviolet imaging: Experimental design and preliminary results," *Coatings*, 11, 6, 2021.

Received: 12-03-2023

Revised: 19-09-2023

Accepted: 15-10-2023